

# BagFormer: Better Cross-Modal Retrieval via bag-wise interaction

Haowen Hou<sup>1</sup>, Xiaopeng Yan<sup>1</sup>, Yigeng Zhang<sup>2</sup>, Fengzong Lian<sup>1</sup> and Zhanhui Kang<sup>1</sup>

<sup>1</sup>Tencent Inc., Shenzhen, China

<sup>2</sup>University of Houston, Houston, USA

haowen.hou@u.nus.edu, chopinyan@tencent.com, yzhang168@uh.edu

## Abstract

In the field of cross-modal retrieval, single encoder models tend to perform better than dual encoder models, but they suffer from high latency and low throughput. In this paper, we present a dual encoder model called BagFormer that utilizes a cross modal interaction mechanism to improve recall performance without sacrificing latency and throughput. BagFormer achieves this through the use of bag-wise interactions, which allow for the transformation of text to a more appropriate granularity and the incorporation of entity knowledge into the model. Our experiments demonstrate that BagFormer is able to achieve results comparable to state-of-the-art single encoder models in cross-modal retrieval tasks, while also offering efficient training and inference with 20.72 times lower latency and 25.74 times higher throughput.

## 1 Introduction

Cross-modal retrieval[Faghri *et al.*, 2017; Zeng *et al.*, 2020] is used for implementing a retrieval task across different modalities(such as image-text or text-image) and is considered one of the most important multimodal understanding tasks[Lee *et al.*, 2018]. The performance of this retrieval task is largely improved by better visual representation and detailed image-text alignment [Cheng *et al.*, 2022]. Recently, cross-modal retrieval has recently been greatly advanced by the development of Vision-Language Pre-Training (VLP), which are capable of learning visual and textual representations from millions of images and texts collected from the Internet and have superior zero-shot ability and robustness[Kim *et al.*, 2021; Lu *et al.*, 2019; Li *et al.*, 2020].

There are mainly two types of cross-modal retrieval architectures: single-encoder and dual-encoder. Single-encoder models like Visual-BERT[Li *et al.*, 2019] and ALBEF[Li *et al.*, 2021] directly feed visual features and textual embeddings to the transformer-based model. Dual-encoder models such as CLIP[Radford *et al.*, 2021] and ALIGN[Jia *et al.*, 2021] have separate encoders for vision and language. In general, dual encoder models are faster but less effective than single encoder models. On the other hand, single-encoder models outperform dual-encoder models in recall metric, but

they are too slow[Khattab and Zaharia, 2020]. Generally speaking, dual-encoder models lack modal interaction and are therefore less effective than single-encoder models[Khattab and Zaharia, 2020]. In this paper, we propose BagFormer, a dual-encoder model with bag-wise interaction mechanism for cross-modal retrieval, which greatly reduces the recall metric gap between the single-encoder models and the dual-encoder models.

Cross-modal interaction and cross-modal alignment of image and text are the key to succeed in cross-modal retrieval[Li *et al.*, 2021; Yao *et al.*, 2021]. In order to achieve fine-grained cross-modal interaction and alignment, previous approaches have mainly based on a two kinds of methods. In a series of works, pre-trained object detectors[Lee *et al.*, 2018; Anderson *et al.*, 2018] have been used to extract ROI features from images and combine them with paired text. This approach can be a bit more challenging since a large number of ROI features must be computed and stored in advance[Li *et al.*, 2021]. Furthermore, the zero-shot ability of these approaches is typically limited by the number of predefined classes, and their performance is also governed by the quality of the detector[Li *et al.*, 2021]. Another series of work introduce interaction between modalities. Single encoder models use token-wise or patch-wise representations and achieves fine-grained interactions via cross-attention or self-attention[Cheng *et al.*, 2022]. However, these methods are typically less efficient in terms of both training and inference. Particularly during training, cross-attention needs to be performed in an encoder-decoder structure, whereas self-attention becomes increasingly complex as it is concatenated with both image and text for extended sequences. For inference, an image-text pair must be combined in order to compute cross-attention or self-attention. Therefore, the single encoder models cannot be pre-computed off-line like dual encoder models, such as CLIP[Radford *et al.*, 2021] and ALIGN[Jia *et al.*, 2021]. Cross-attention or self-attention used in single encoder models is too expensive in computation, so CoBERT[Khattab and Zaharia, 2020; Santhanam *et al.*, 2021] proposes to introduce a late interaction mechanism into the dual encoder models to achieve efficient and effective passage retrieval. FILIP[Yao *et al.*, 2021] introduces the idea of late interaction into the multi-modal domain.

Our paper aims to optimize the cross-modal interaction so that the dual encoder model’s performance is close to the

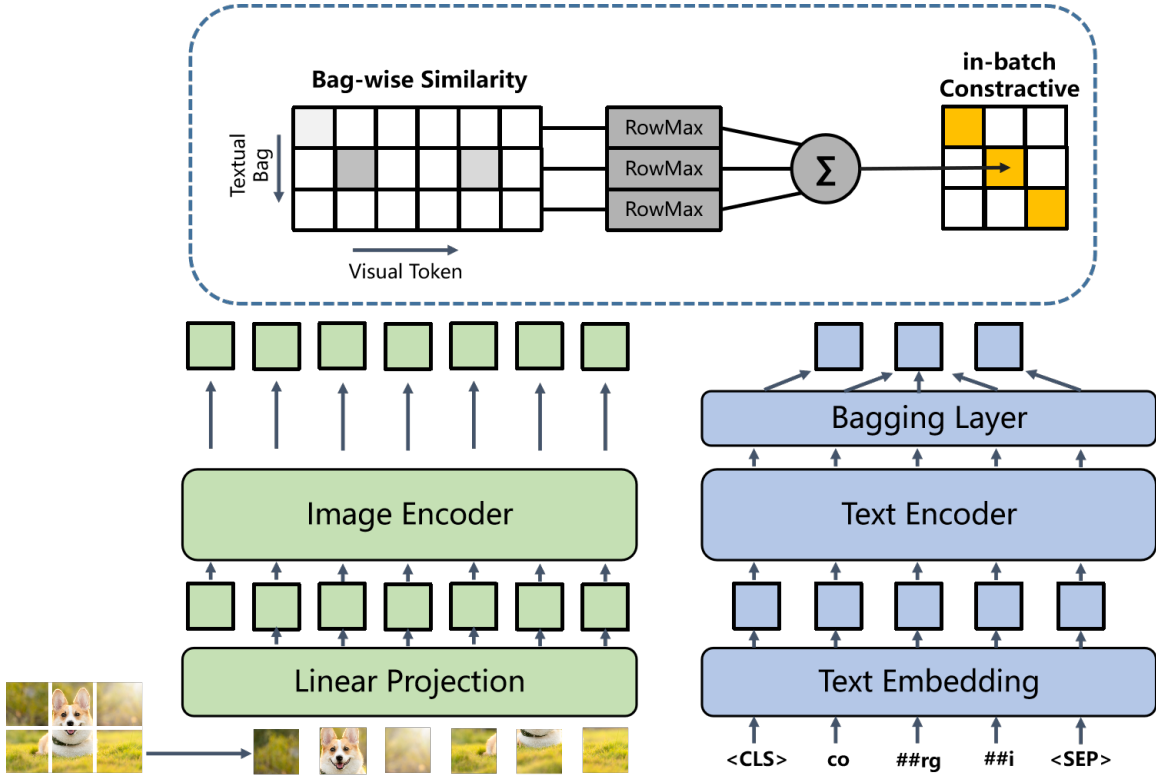


Figure 1: The architecture of BagFormer network. A Dual-encoder architecture with Transformer-based image encoder and text encoder. Textual tokens in a ‘bag’ are aggregated to textual bags by the bagging layer. Then the representations of textual bags and visual tokens are linearly projected into the multi-modal joint space. We propose a novel bag-wise interaction method based on bag-wise maximum similarity between visual tokens and textual bags.

single encoder model’s with significantly lower latency and higher throughput. To this end, we propose BagFormer, a dual encoder model with bag-wise interaction to achieve better cross modal interaction and alignment. The BagFormer adopts the bag-wise interaction mechanism, which can transform text to appropriate granularity and implicitly introduce entity knowledge into the model. More specifically, BagFormer uses a bag-wise maximum similarity between visual and textual tokens to guide the contrastive objective. In this way, BagFormer successfully leverages the fine-grained expressiveness among image patches and textual words while simultaneously gaining the ability to pre-compute image and text representations off-line.

Several experiments have demonstrated that BagFormer’s learning of bag representations allows it to perform at the top of its class. On image-text retrieval, BagFormer performs almost as well as the state of the art single encoder model, but the latency is reduced by 20.72 times, and the throughput is increased by 25.74 times. In addition, BagFormer outperforms other dual encoder models that are pre-trained on larger datasets. Furthermore, visualizations of word patch alignment demonstrate BagFormer is able to learn meaningful fine-grained features with promising localization capabilities.

## 2 Related Work

**Vision language pre-training.** As a mainstream paradigm in multi-modal understanding, vision language pre-training has significantly increased performance on various vision and language tasks. The majority of these approaches use transformer-based architectures, which can be categorized as single-encoder and dual-encoder. With single encoder architectures, such as ALBEF[Li *et al.*, 2021], multi-modal transformers can simultaneously process images and text for high-performance interactions. The computation cost of these approaches, however, is still impractical for large-scale cross-modal retrieval tasks. In contrast, dual encoder architectures, such as CLIP[Radford *et al.*, 2021] and ALIGN[Jia *et al.*, 2021], encode images and text separately, making it possible to calculate image-text similarities in linear time. Although the million-scale image-text contrastive pre-training greatly improves the dual encoder architecture, a performance gap still exists between it and single encoder architecture. By contrast, BagFormer incorporates bag-wise interaction into dual encoder architecture, reducing performance gap while increasing inference speed.

**Dense retrieval.** Dense retrieval involves using dense vectors to represent queries and documents and using techniques such as inner product or cosine similarity to measure their similarity[Wang *et al.*, 2022]. This research area has recently been advanced by the use of pre-trained language

models like BERT[Devlin *et al.*, 2018] and RoBERTa[Liu *et al.*, 2019], which can generate dense representations for queries and documents. To efficiently search for relevant documents, approximate nearest neighbor algorithms such as k-dimensional trees[Bentley, 1975], locality-sensitive hashing[Datar *et al.*, 2004], and graph-based indexes[Malkov and Yashunin, 2018] can be utilized to retrieve documents in sublinear time. In addition, ColBERT[Khattab and Zaharia, 2020] and ColBERTv2[Santhanam *et al.*, 2021] developed a late interaction paradigm that uses a scalable "MaxSim" operator for query-document interaction to boost search quality.

**Cross-modal retrieval.** Cross-modal retrieval is the task of retrieving relevant images or text descriptions given a text or image query. In recent years, the visual representation for cross-modal retrieval has been improved through the use of techniques such as grid-based CNNs[Faghri *et al.*, 2017], pre-trained object detectors[Anderson *et al.*, 2018] and vision-language pre-training models[Radford *et al.*, 2021]. At the same time, there have been advances in methods for aligning images and text, including the use of attention mechanisms[Li *et al.*, 2021], iterative matching[Chen *et al.*, 2020], graph-based relationship reasoning[Liu *et al.*, 2020] and late interaction mechanism[Khattab and Zaharia, 2020]. FILIP[Yao *et al.*, 2021] borrow this idea of late interaction mechanism from ColBERT[Khattab and Zaharia, 2020], and develop a token-wise interaction for better cross-modal retrieval. BagFormer takes this approach a step further by introducing the idea of bag-wise interactions.

### 3 BagFormer

#### 3.1 Model Architecture

**Model Architecture.** BagFormer integrates an image encoder based on a 12-layer visual transformer (ViT-B/16)[Dosovitskiy *et al.*, 2020] with weights pre-trained on ImageNet-1k[Touvron *et al.*, 2021] and a text encoder based on a 6-layer transformer[Vaswani *et al.*, 2017] initialised with the first 6 layers of the BERT-base[Devlin *et al.*, 2018] model. The input image and text are converted into respective sequences of visual embeddings  $\{v_{cls}, v_1, \dots, v_n\}$  and token embeddings  $\{t_{cls}, t_1, \dots, t_m\}$ . These embeddings are then projected into a common multimodal space via linear transformation, and subsequently normalised using L2-normalisation. Finally, the token embeddings are aggregated to form bag embeddings via the bagging layer, and the bag-wise similarity is then calculated by the late interaction of the visual embeddings and bag embeddings.

#### 3.2 Pre-training Objectives

The two objectives of BagFormer’s pre-training are image-text contrastive learning (ITC) and bag-wise contrastive learning (BWC).

**Image-Text Contrastive Learning** aims to align the global representations of image and text. In CLIP[Radford *et al.*, 2021], [CLS] token of image patches and text tokens are used to compute the global feature, and the similarity is computed via the dot product of the global feature. More specifically, the global similarity between the image and the

text is computed as follows:

$$s(I, T) = s(T, I) = g_v(v_{cls})^T g_t(t_{cls}) \quad (1)$$

where  $g_v(v_{cls})$  denotes the embedding of the [CLS] token of the image and  $g_t(v_{cls})$  denotes the embedding of the [CLS] token of the text.  $g_v$  is the visual projection head and  $g_t$  is the textual projection head.

For each image and text, we calculate the image-to-text and text-to-image contrastive loss as

$$L_{i2t} = -\frac{1}{bs} \log \frac{\exp(s(I, T)/\tau)}{\sum_{n=1}^{bs} \exp(s(I, T)/\tau)} \quad (2)$$

$$L_{t2i} = -\frac{1}{bs} \log \frac{\exp(s(T, I)/\tau)}{\sum_{n=1}^{bs} \exp(s(T, I)/\tau)} \quad (3)$$

where  $\tau$  is a learnable temperature parameter and  $bs$  is the batch size. The total image-text contrastive loss of one training batch is then computed as follows:

$$L_{itc} = \frac{1}{2} (L_{t2i} + L_{i2t}) \quad (4)$$

**Bag-wise Contrastive Learning.** Bag-wise Contrastive Learning is based on the bag-wise similarity, which is computed using a fine-grained interaction between image patches and text bags. A text bag is calculated by summing the embeddings of text tokens in a 'bag'. The bagging layer transforms the last-layer token embeddings  $\{t_{cls}, t_1, \dots, t_m\}$  into a sequence of bag embeddings  $\{b_{cls}, b_1, \dots, b_k\}$ . Each visual token  $g_v(v_i)$  computes similarities with all non-padded textual bags, followed by selecting the maximum value of these similarities as the activation of that visual token. Finally, we average the activation of all visual tokens as the bag-wise image-to-text similarity.

$$s(I, T)_{bag} = \frac{1}{n} \sum_{i=1}^n \max(g_v(v_i)^T g_t(b_1 \dots b_k)) \quad (5)$$

where  $n$  is the sequence length of image patches and  $k$  is the sequence length of text bags. The bag-wise text-to-image similarity can be computed in the same way.

#### 3.3 Bagging Layer

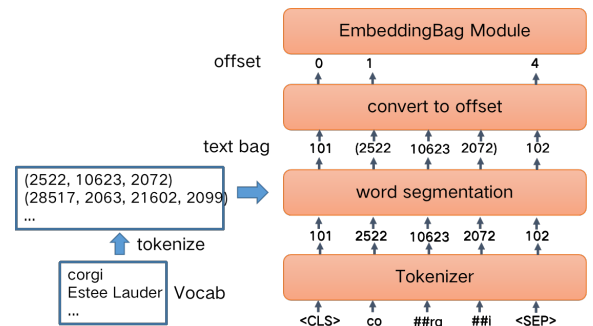


Figure 2: An illustration of the bagging layer.

The purpose of bagging layer is to adjust the token granularity through by aggregating tokens into a bag, which can

be a word, an entity or a phrase. At the same time, the bagging layer is able to implicitly add a priori knowledge from the vocabulary to the model for better alignment for text and images. The vocabulary is a very useful priori knowledge that can be plugged into the model to enhance it. Vocabulary can be gathered manually or through data mining algorithms, such as AutoPhrase[Shang *et al.*, 2018].

The workflow of the bagging layer can be divided into 3 steps. The first step is to train a bagging helper, which will store the index of tokenized word/entity/phrase. In the second step, with the help of word segmentation algorithm, the input token index will be bagged in a 'bag'. In the last step, the index bag will be converted to offset, which will be fed into EmbeddingBag module. EmbeddingBag module is a high efficient implement for summing of 'bags' of embeddings, without instantiating the intermediate embeddings. Finally, we have a sequence of bag embedding as the layer's output.

### 3.4 Early bagging vs. Late bagging

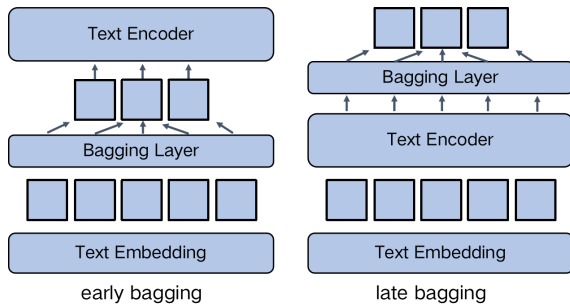


Figure 3: Early bagging architecture(left) and late bagging Architecture(right).

Two architectures were designed for BagFormer: an early bagging architecture and a late bagging architecture. As shown in Figure 3, the text tokens are bagged before the text encoder in the early bagging architecture. For the late bagging architecture, all tokens are bagged after passing through the text encoder. According to the results, the late bagging architecture outperforms the early bagging architecture, which we will discuss in next section.

### 3.5 Implementation Details

Text encoder is a 6-layer BERT model with 58.3M parameters and image encoder is a 12-layer visual transformer ViT-B/16 with 85.8M parameters. Following [Radford *et al.*, 2021], we tokenize the text using byte pair encoding (BPE)[Sennrich *et al.*, 2015].

## 4 Experiments

### 4.1 Experimental Setup

**Pre-training Dataset.** Our pre-training dataset consists 108M image-text pairs, collected from the web. Average length of text is 25 words.

**Experiment Details.** We pre-train the model for 15 epochs using a batch size of 512 on 8 NVIDIA V100 GPUs. AdamW[Loshchilov and Hutter, 2017] optimizer is used with

a weight decay of 0.02. Following a cosine schedule, the learning rate is warmed up to  $1e^{-4}$  in the first 2000 iterations, then decayed to  $1e^{-5}$ . Random cropped images of  $256 \times 256$  resolution and RandAugment[Cubuk *et al.*, 2020] are used as inputs during pre-training. During fine-tuning, we keep the image resolution at  $256 \times 256$ . During inference, we resize the images without cropping them. In addition, we constructed a vocabulary of 342,729 entities for the bagging layer.

### 4.2 Modal Granularity Mismatch

Our experiments have observed a discrepancy in performance between text-to-image recall and image-to-text recall in cross-modal retrieval. In Table 1 and Table 2, we see that the image-to-text retrieval performance of the CLS token model(w/o late interaction) and the tokenwise interaction model(w/o bagging layer) is significantly lower than their text-to-image retrieval performance. However, the image-to-text retrieval performance of the BagFormer model is significantly better than the control group(model w/o late interaction and model w/o bagging layer). We can conclude that the improved performance of the BagFormer model is mainly due to its improved image-to-text retrieval task.

Our findings indicate that the poor performance of the CLS token model (without late interaction) and the tokenwise interaction model (without a bagging layer) is primarily due to a granularity mismatch between the image and the text. This is especially true in languages such as Chinese, in which token granularity is not sufficient to convey the complete semantics. BagFormer attempts to solve this problem by converting token granularity into bags of words or entities to enable better alignment between the text and the images. The success of BagFormer is largely attributed to its ability to alleviate the modal granularity mismatch.

### 4.3 Image-Text Retrieval

In this section, we test our models on two subtasks: image-to-text retrieval and text-to-image retrieval. In the image-to-text retrieval, the model retrieves a target text from a set of candidates given an image as query, or vice versa for the text-to-image retrieval. We evaluate our BagFormer on three retrieval benchmark datasets, including Flickr30K-CNA[Xie *et al.*, 2022], MUGE[Lin *et al.*, 2021] and Wukong50K[Gu *et al.*, 2022], under both zero-shot and fine-tuned settings. Due to the lack of a training set, Wukong50K is used only in zero-shot setting.

Our pre-trained models are evaluated in zero-shot and fine-tuned settings for each dataset. In accordance with common practices, we report Recall@K (recall of the top K candidates) with  $K = 1, 5, 10$  for both image-to-text retrieval and text-to-image retrieval across all datasets. In the final comparison, the mean recall (MR) of Recall@K is used. Results are reported for the test sets, except for MUGE, where there are no test set available. For that case, we report results from the MUGE validation set.

Table 1 and Table 2 summarize the results of the zero-shot and fine-tuned image-text retrieval respectively. ALBEF is a very strong benchmark for single-tower model, which has

| Dataset       | Method                  | Image-to-Text Retrieval |              |              | Text-to-Image Retrieval |              |              | MR           |
|---------------|-------------------------|-------------------------|--------------|--------------|-------------------------|--------------|--------------|--------------|
|               |                         | R@1                     | R@5          | R@10         | R@1                     | R@5          | R@10         |              |
| Flickr30k-CNA | <b>BagFormer(Base)</b>  | <b>4.10</b>             | <b>15.90</b> | <b>23.20</b> | <b>5.02</b>             | <b>13.94</b> | <b>20.62</b> | <b>13.79</b> |
|               | w/o bagging layer       | 1.00                    | 5.30         | 8.70         | 4.04                    | 12.22        | 18.02        | 8.21         |
|               | w/o late interaction    | 0.10                    | 0.50         | 1.40         | 0.76                    | 3.04         | 5.54         | 1.89         |
| Wukong50k     | <b>BagFormer(Base)</b>  | <b>10.53</b>            | <b>18.50</b> | <b>22.12</b> | <b>18.61</b>            | <b>30.06</b> | <b>34.14</b> | <b>22.33</b> |
|               | w/o bagging layer       | 4.31                    | 10.91        | 14.68        | 17.46                   | 28.60        | 32.75        | 18.12        |
|               | w/o late interaction    | 0.07                    | 0.18         | 0.32         | 11.31                   | 19.64        | 23.42        | 9.16         |
| MUGE          | ALBEF                   | 30.81                   | 57.74        | 67.94        | 43.01                   | 68.73        | 77.17        | 57.57        |
|               | Wukong <sub>ViT-B</sub> | -                       | -            | -            | 33.40                   | 59.30        | 69.70        | -            |
|               | <b>BagFormer(Base)</b>  | <b>31.11</b>            | <b>57.65</b> | <b>67.57</b> | <b>40.73</b>            | <b>67.61</b> | <b>76.59</b> | <b>56.88</b> |
|               | w/o bagging layer       | 2.52                    | 8.91         | 15.48        | 37.50                   | 64.39        | 74.04        | 33.81        |
|               | w/o late interaction    | 1.08                    | 3.69         | 5.89         | 19.05                   | 39.15        | 49.02        | 19.65        |

Table 1: Ablation study of zero-shot image-text retrieval on several datasets.

| Dataset       | Method                  | Image-to-Text Retrieval |              |              | Text-to-Image Retrieval |              |              | MR           |
|---------------|-------------------------|-------------------------|--------------|--------------|-------------------------|--------------|--------------|--------------|
|               |                         | R@1                     | R@5          | R@10         | R@1                     | R@5          | R@10         |              |
| Flickr30k-CNA | <b>BagFormer(Base)</b>  | <b>66.0</b>             | <b>87.1</b>  | <b>92.4</b>  | <b>48.19</b>            | <b>76.75</b> | <b>85.51</b> | <b>75.99</b> |
|               | w/o bagging layer       | 35.6                    | 65.6         | 78.6         | 44.35                   | 73.89        | 82.97        | 63.50        |
|               | w/o late interaction    | 27.4                    | 58.5         | 72.2         | 30.19                   | 59.28        | 70.32        | 52.98        |
| MUGE          | ALBEF                   | 41.86                   | 72.78        | 82.27        | 53.05                   | 80.47        | 87.48        | 69.65        |
|               | Wukong <sub>ViT-B</sub> | -                       | -            | -            | 39.20                   | 66.90        | 77.40        | -            |
|               | <b>BagFormer(Base)</b>  | <b>41.23</b>            | <b>72.06</b> | <b>81.10</b> | <b>52.41</b>            | <b>79.19</b> | <b>86.54</b> | <b>68.75</b> |
|               | w/o bagging layer       | 11.34                   | 30.14        | 41.18        | 47.20                   | 75.69        | 84.42        | 48.33        |
|               | w/o late interaction    | 21.29                   | 51.16        | 65.24        | 46.44                   | 75.28        | 84.36        | 57.29        |

Table 2: Ablation study of fine-tuned image-text retrieval on several datasets.

the highest results in MUGE dataset. The result of our BagFormer achieve comparable performance to state-of-the-art model ALBEF, while significantly higher than another benchmark model Wukong<sub>ViT-B</sub>, across different datasets, in either zero-shot or fine-tuned settings. In comparison to ALBEF, our dual tower BagFormer, which has comparable performance.

#### 4.4 Ablation Study

Additionally, we conducted ablation studies as shown in table 1 and table 2. BagFormer w/o bagging layer remove the bagging layer but keep the late interaction, which is the token-wise model as in ColBERT[Khattab and Zaharia, 2020] and FILIP[Yao *et al.*, 2021]. BagFormer w/o late interaction remove both the bagging layer and late interaction loss, which is similar to CLIP[Radford *et al.*, 2021].

As shown in ablation studies, these improvements are owing to the novel designs of bagging layer and late interaction. We also notice that bagging layer plays a key role in boosting the retrieval performance. The main improvement comes from Image-to-Text retrieval task, which alleviate the modal granularity mismatch.

#### 4.5 Efficiency Analysis

The efficiency of BagFormer was evaluated using an NVIDIA T4-16G GPU. Latency and throughput of the model were assessed in a re-ranking setting, in which each query is paired

with the top 64 candidates and rescored by the model. The results, as presented in Table 4, demonstrate that BagFormer has a significantly shorter latency (20.72 times shorter) and higher throughput (25.74 times higher) compared to the single encoder architecture, which use ALBEF as the feature extractor and 6-layer transformer to fuse multimodal features. Additionally, while BagFormer is slightly slower than the dual encoder architecture, in which ALBEF was used as the feature extractor and the CLS token similarity was employed for scoring, it demonstrates much higher recall metrics.

#### 4.6 Early bagging vs. Late bagging

The early bagging and late bagging architectures were tested on the MUGE dataset[Lin *et al.*, 2021]. Table 3 shows that late bagging architecture generally outperforms early bagging architecture on cross-modal retrieval tasks. In zero-shot results, the late bagging architecture performed better than the early bagging architecture, indicating that it can help the model to obtain better text-image alignment during pre-training. Compared with early bagging architecture, the reason why late bagging architecture is better may be that there is less information loss and better use of prior information provided by external knowledge.

#### 4.7 Visualization of cross-modal alignment

The following section examines BagFormer’s ability to capture fine-grained cross-modal alignment. Due to a lack of



| Setting    | Method                             | Image-to-Text Retrieval |       |       | Text-to-Image Retrieval |       |       | MR    |
|------------|------------------------------------|-------------------------|-------|-------|-------------------------|-------|-------|-------|
|            |                                    | R@1                     | R@5   | R@10  | R@1                     | R@5   | R@10  |       |
| Zero-shot  | BagFormer <sub>early-bagging</sub> | 19.83                   | 34.22 | 38.97 | 40.31                   | 67.95 | 76.87 | 46.36 |
|            | BagFormer <sub>bagwise</sub>       | 31.11                   | 57.65 | 67.57 | 40.73                   | 67.61 | 76.59 | 56.88 |
| Fine-tuned | BagFormer <sub>early-bagging</sub> | 39.61                   | 67.60 | 74.75 | 51.61                   | 77.75 | 85.12 | 66.07 |
|            | BagFormer <sub>bagwise</sub>       | 41.23                   | 72.06 | 81.10 | 52.41                   | 79.19 | 86.54 | 68.75 |

Table 3: Results of image-text retrieval for early and late bagging on the MUGE dataset.

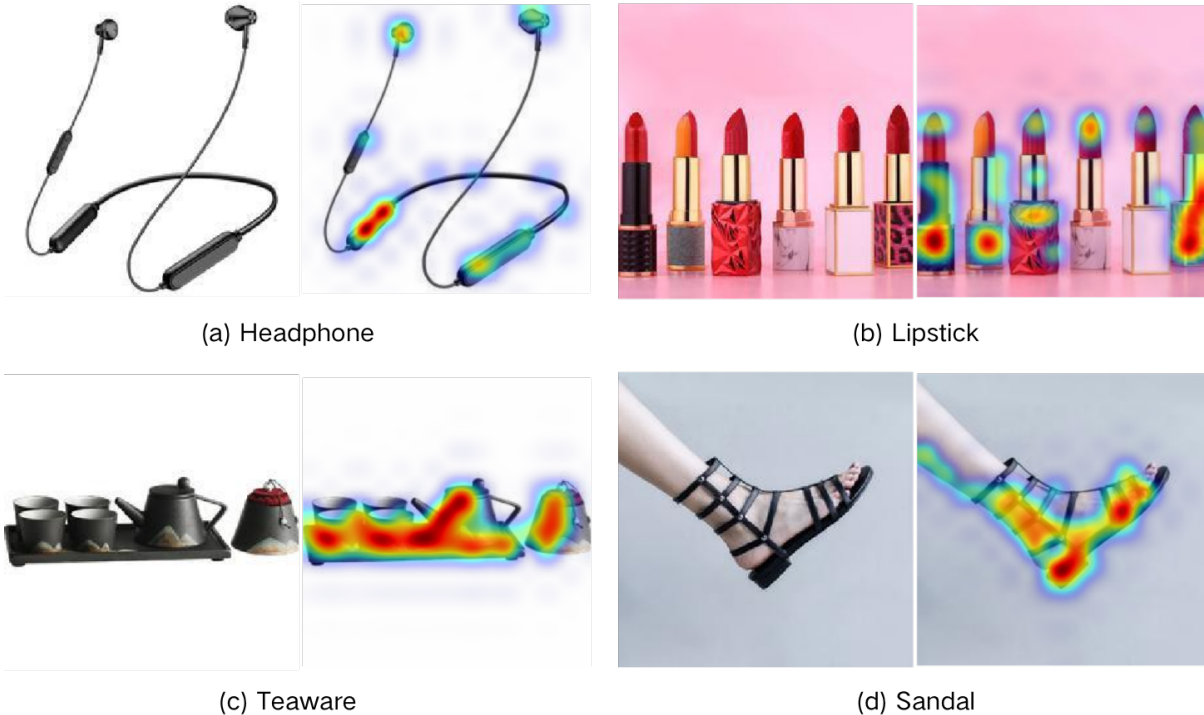


Figure 4: Word-patch visualizations on the bag-wise similarity maps.

| Method                          | Latency (ms) | Throughput (queries/s) |
|---------------------------------|--------------|------------------------|
| All-to-all interaction          | 840.80       | 1.26                   |
| Representation-based similarity | 40.41        | 29.30                  |
| Bag-wise interaction            | 40.57        | 27.03                  |

Table 4: Efficiency analysis.

word-patch alignment capability, the visualization of CLIP is excluded[Yao *et al.*, 2021]. As shown in Figure 4, we visualize four images with word-bag in the MUGE dataset. The visualization is performed based on the bag-wise similarity between the image patches and textual bags. Specifically, we calculate the bag-wise similarity between image patches and word bag to produce a heat map that shows the word bag’s activation.

As shown in the Figure 4, BagFormer can learn meaningful fine-grained features and demonstrate promising localization

abilities. BagFormer can outline the teaware in the example of Figure 4 (c), while BagFormer often aligns to the key part of the target object in the examples of Figure 4 (a,b,d).

## 5 Conclusion

In this paper, we introduce BagFormer, a dual encoder model with novel bag-wise interaction mechanism. The proposed BagFormer leverage bag-wise interaction mechanism, which introduce appropriate granularity to text and implicitly introduce entity knowledge. Through empirical evaluation on the MUGE, Flickr30k-CNA, and Wukong50k datasets, we demonstrate that BagFormer is capable of achieving performance comparable to that of a single tower model, but with significantly lower latency (20.7 times) and higher throughput (25.74 times).

## Ethical Statement

There are no ethical issues.

## References

- [Anderson *et al.*, 2018] Peter Anderson, Xiaodong He, Chris Buehler, Damien Teney, Mark Johnson, Stephen Gould, and Lei Zhang. Bottom-up and top-down attention for image captioning and visual question answering. In *Proceedings of the IEEE conference on computer vision and pattern recognition*, pages 6077–6086, 2018.
- [Bentley, 1975] Jon Louis Bentley. Multidimensional binary search trees used for associative searching. *Communications of the ACM*, 18(9):509–517, 1975.
- [Chen *et al.*, 2020] Hui Chen, Guiguang Ding, Xudong Liu, Zijia Lin, Ji Liu, and Jungong Han. Imram: Iterative matching with recurrent attention memory for cross-modal image-text retrieval. In *Proceedings of the IEEE/CVF conference on computer vision and pattern recognition*, pages 12655–12663, 2020.
- [Cheng *et al.*, 2022] Mengjun Cheng, Yipeng Sun, Longchao Wang, Xiongwei Zhu, Kun Yao, Jie Chen, Guoli Song, Junyu Han, Jingtuo Liu, Errui Ding, et al. Vista: Vision and scene text aggregation for cross-modal retrieval. In *Proceedings of the IEEE/CVF Conference on Computer Vision and Pattern Recognition*, pages 5184–5193, 2022.
- [Cubuk *et al.*, 2020] Ekin D Cubuk, Barret Zoph, Jonathon Shlens, and Quoc V Le. Randaugment: Practical automated data augmentation with a reduced search space. In *Proceedings of the IEEE/CVF conference on computer vision and pattern recognition workshops*, pages 702–703, 2020.
- [Datar *et al.*, 2004] Mayur Datar, Nicole Immorlica, Piotr Indyk, and Vahab S Mirrokni. Locality-sensitive hashing scheme based on p-stable distributions. In *Proceedings of the twentieth annual symposium on Computational geometry*, pages 253–262, 2004.
- [Devlin *et al.*, 2018] Jacob Devlin, Ming-Wei Chang, Kenton Lee, and Kristina Toutanova. Bert: Pre-training of deep bidirectional transformers for language understanding. *arXiv preprint arXiv:1810.04805*, 2018.
- [Dosovitskiy *et al.*, 2020] Alexey Dosovitskiy, Lucas Beyer, Alexander Kolesnikov, Dirk Weissenborn, Xiaohua Zhai, Thomas Unterthiner, Mostafa Dehghani, Matthias Minderer, Georg Heigold, Sylvain Gelly, et al. An image is worth 16x16 words: Transformers for image recognition at scale. *arXiv preprint arXiv:2010.11929*, 2020.
- [Faghri *et al.*, 2017] Fartash Faghri, David J Fleet, Jamie Ryan Kiros, and Sanja Fidler. Vse++: Improving visual-semantic embeddings with hard negatives. *arXiv preprint arXiv:1707.05612*, 2017.
- [Gu *et al.*, 2022] Jiayi Gu, Xiaojun Meng, Guansong Lu, Lu Hou, Minzhe Niu, Hang Xu, Xiaodan Liang, Wei Zhang, Xin Jiang, and Chunjing Xu. Wukong: 100 million large-scale chinese cross-modal pre-training dataset and a foundation framework. *arXiv preprint arXiv:2202.06767*, 2022.
- [Jia *et al.*, 2021] Chao Jia, Yinfei Yang, Ye Xia, Yi-Ting Chen, Zarana Parekh, Hieu Pham, Quoc Le, Yun-Hsuan Sung, Zhen Li, and Tom Duerig. Scaling up visual and vision-language representation learning with noisy text supervision. In *International Conference on Machine Learning*, pages 4904–4916. PMLR, 2021.
- [Khattab and Zaharia, 2020] Omar Khattab and Matei Zaharia. Colbert: Efficient and effective passage search via contextualized late interaction over bert. In *Proceedings of the 43rd International ACM SIGIR conference on research and development in Information Retrieval*, pages 39–48, 2020.
- [Kim *et al.*, 2021] Wonjae Kim, Bokyoung Son, and Ildoo Kim. Vilt: Vision-and-language transformer without convolution or region supervision. In *International Conference on Machine Learning*, pages 5583–5594. PMLR, 2021.
- [Lee *et al.*, 2018] Kuang-Huei Lee, Xi Chen, Gang Hua, Houdong Hu, and Xiaodong He. Stacked cross attention for image-text matching. In *Proceedings of the European conference on computer vision (ECCV)*, pages 201–216, 2018.
- [Li *et al.*, 2019] Liunian Harold Li, Mark Yatskar, Da Yin, Cho-Jui Hsieh, and Kai-Wei Chang. Visualbert: A simple and performant baseline for vision and language. *arXiv preprint arXiv:1908.03557*, 2019.
- [Li *et al.*, 2020] Gen Li, Nan Duan, Yuejian Fang, Ming Gong, and Daxin Jiang. Unicoder-vl: A universal encoder for vision and language by cross-modal pre-training. In *Proceedings of the AAAI Conference on Artificial Intelligence*, volume 34, pages 11336–11344, 2020.
- [Li *et al.*, 2021] Junnan Li, Ramprasaath Selvaraju, Akhilesh Gotmare, Shafiq Joty, Caiming Xiong, and Steven Chu Hong Hoi. Align before fuse: Vision and language representation learning with momentum distillation. *Advances in neural information processing systems*, 34:9694–9705, 2021.
- [Lin *et al.*, 2021] Junyang Lin, Rui Men, An Yang, Chang Zhou, Ming Ding, Yichang Zhang, Peng Wang, Ang Wang, Le Jiang, Xianyan Jia, et al. M6: A chinese multi-modal pretrainer. *arXiv preprint arXiv:2103.00823*, 2021.
- [Liu *et al.*, 2019] Yinhan Liu, Myle Ott, Naman Goyal, Jingfei Du, Mandar Joshi, Danqi Chen, Omer Levy, Mike Lewis, Luke Zettlemoyer, and Veselin Stoyanov. Roberta: A robustly optimized bert pretraining approach. *arXiv preprint arXiv:1907.11692*, 2019.
- [Liu *et al.*, 2020] Chunxiao Liu, Zhendong Mao, Tianzhu Zhang, Hongtao Xie, Bin Wang, and Yongdong Zhang. Graph structured network for image-text matching. In *Proceedings of the IEEE/CVF conference on computer vision and pattern recognition*, pages 10921–10930, 2020.
- [Loshchilov and Hutter, 2017] Ilya Loshchilov and Frank Hutter. Decoupled weight decay regularization. *arXiv preprint arXiv:1711.05101*, 2017.

- [Lu *et al.*, 2019] Jiasen Lu, Dhruv Batra, Devi Parikh, and Stefan Lee. Vilbert: Pretraining task-agnostic visiolinguistic representations for vision-and-language tasks. *Advances in neural information processing systems*, 32, 2019.
- [Malkov and Yashunin, 2018] Yu A Malkov and Dmitry A Yashunin. Efficient and robust approximate nearest neighbor search using hierarchical navigable small world graphs. *IEEE transactions on pattern analysis and machine intelligence*, 42(4):824–836, 2018.
- [Radford *et al.*, 2021] Alec Radford, Jong Wook Kim, Chris Hallacy, Aditya Ramesh, Gabriel Goh, Sandhini Agarwal, Girish Sastry, Amanda Askell, Pamela Mishkin, Jack Clark, et al. Learning transferable visual models from natural language supervision. In *International Conference on Machine Learning*, pages 8748–8763. PMLR, 2021.
- [Santhanam *et al.*, 2021] Keshav Santhanam, Omar Khattab, Jon Saad-Falcon, Christopher Potts, and Matei Zaharia. Colbertv2: Effective and efficient retrieval via lightweight late interaction. *arXiv preprint arXiv:2112.01488*, 2021.
- [Sennrich *et al.*, 2015] Rico Sennrich, Barry Haddow, and Alexandra Birch. Neural machine translation of rare words with subword units. *arXiv preprint arXiv:1508.07909*, 2015.
- [Shang *et al.*, 2018] Jingbo Shang, Jialu Liu, Meng Jiang, Xiang Ren, Clare R Voss, and Jiawei Han. Automated phrase mining from massive text corpora. *IEEE Transactions on Knowledge and Data Engineering*, 30(10):1825–1837, 2018.
- [Touvron *et al.*, 2021] Hugo Touvron, Matthieu Cord, Matthijs Douze, Francisco Massa, Alexandre Sablayrolles, and Hervé Jégou. Training data-efficient image transformers & distillation through attention. In *International Conference on Machine Learning*, pages 10347–10357. PMLR, 2021.
- [Vaswani *et al.*, 2017] Ashish Vaswani, Noam Shazeer, Niki Parmar, Jakob Uszkoreit, Llion Jones, Aidan N Gomez, Łukasz Kaiser, and Illia Polosukhin. Attention is all you need. *Advances in neural information processing systems*, 30, 2017.
- [Wang *et al.*, 2022] Yujing Wang, Yingyan Hou, Haonan Wang, Ziming Miao, Shibin Wu, Hao Sun, Qi Chen, Yuqing Xia, Chengmin Chi, Guoshuai Zhao, et al. A neural corpus indexer for document retrieval. *arXiv preprint arXiv:2206.02743*, 2022.
- [Xie *et al.*, 2022] Chunyu Xie, Heng Cai, Jianfei Song, Jincheng Li, Fanjing Kong, Xiaoyu Wu, Henrique Morimitsu, Lin Yao, Dexin Wang, Dawei Leng, et al. Zero and r2d2: A large-scale chinese cross-modal benchmark and a vision-language framework. *arXiv preprint arXiv:2205.03860*, 2022.
- [Yao *et al.*, 2021] Lewei Yao, Runhui Huang, Lu Hou, Guan-song Lu, Minzhe Niu, Hang Xu, Xiaodan Liang, Zhen-guo Li, Xin Jiang, and Chunjing Xu. Filip: Fine-grained interactive language-image pre-training. *arXiv preprint arXiv:2111.07783*, 2021.
- [Zeng *et al.*, 2020] Donghuo Zeng, Yi Yu, and Keizo Oyama. Deep triplet neural networks with cluster-cca for audio-visual cross-modal retrieval. *ACM Transactions on Multimedia Computing, Communications, and Applications (TOMM)*, 16(3):1–23, 2020.